[1]Y. P. Arul Teen

[2]Anchana BS

[3]Nimmy Lazer

[4]Diffia W

Advanced Ingestible Sensor Pills for Real-Time Digestive System and Hydration Monitoring Using CLSTM Data Analysis

JES Journal of Electrical Systems

Abstract: From intrusive implanted devices to more approachable exterior and edible technology, wearable sensors have attracted a number of customers. Implantable devices that are extremely expensive and invasive, which restricts their use even though they offer vital life support. Conversely, ingestible sensors with pills present a more cost-effective and minimally intrusive alternative. This work introduces a unique ingestible sensor that can track real-time electrolyte balance and hydration leveling's in addition to gastrointestinal health parameters including gut motility and pH levels. To analyze the sensor data, we utilised a novel Concatenated Long Short-Term Memory (CLSTM) deep learning algorithm. This allows the users to accurately identify electrolytic imbalance and dehydrating stages early on, as well as the gastrointestinal diseases like Crohn's disease and irritable bowel syndromes. The proposed results gives that our adaptable edible sensor has been a useful tool for managing gastrointestinal health as well as optimizing hydration because it not only offers thorough health in detections but also makes proper actions easier. This strategy is having the potential to improve overall health management, tailored treatment and early detection in a variety of groups.

Keywords: Sensors, Ingestible technology, Electrolyte balance, Hydration monitoring, Gastrointestinal health and Deep learning algorithms.

1. INTRODUCTION

When ingestable electronics first emerged in the 1950s, the capacity to measure pressure, temperature, and pH was substantiated by clinical proof-of-concept experiments. The initial ingestible temperature sensors

[1]Assistant Professor
Department: Electronics and Communication Engineering
University College of Engineering
Nagercoil, Kanyakumari, Tamilnadu, India
arulteen@gmail.com
[2]Assistant Professor
Department: Computer Science Engineering
Ponjesly college of Engineering,
Nagercoil, Kanyakumari, Tamilnadu, India
anchana.bs@gmail.com
[3]Associate Professor
Department:Electronics and Communication Engineering
Saveetha School of Engineering,
Kanchipuram, Tamilnadu, India
nimmylazer.sse@saveetha.com
[4]Research Scholar
Department:Electronics and Communication Engineering
Institute: University College of Engineering
Nagercoil, Kanyakumari, Tamilnadu, India
diffia.w.1996@gmail.com

were developed in the 1980s and 1990s as a consequence of further advancements, and the first video capsule endoscopic system was developed shortly thereafter [1]. Research on edible electrical devices is still ongoing and has not stopped being developed.

The fundamental signals that guide clinical judgment in a variety of situations are represented by vital signs. This article describes the development of a vitals-monitoring tablet (VM pill; Figure 1) that monitors both respiratory rate (RR) and heart rate (HR) [2]. Having acknowledged the capacity to see these factors, we have used them in two contexts that represent significant clinical barriers: opioid-induced respiratory depression (OIRD) in conjunction with polysomnography in (PSG; sleep study) evaluation [3].

According to preliminary statistics from the CDC [4], 109,680 individuals have perished as the opioid epidemic becomes worse. In reaction to the announcement that drug-related deaths in the country reached a record high in 2022, this report was issued. The number of drug-related fatalities has increased even after a presidential decree was issued in 2017 establishing the President's Commission on preventing Drug Addiction with the Opioids Crisis. 33,091 catastrophic and avoidable opioid overdoses were recorded in 2015; the United States Centers for Chronic Disease Control (CDC) and Prevent National Center for Information on Health referred to this amount as an epidemic. As a direct result of this investigation, the Commission of the President and the Stanford-Lancet Commission were founded in 2021. Both committees insisted on the development of a synthetic opioid antagonist delivery system that may be activated automatically in cases when a patient shows symptoms of opioid receptor malfunction. 63% of opioid overdoses happen when the victim is alone themselves, which is a significant statistic. In [5] OIRD, which is caused by an overdose of opioids, may prove fatal or be linked to issues related to hypoxia, such as damage to organ systems, cardiac arrest, stroke, even psychosis. The recommended course of treatment for reversing OIRD is opioid antagonists. Even though more people have access to opioid antagonists, which has decreased the number of opioid-related deaths [6], 70% of people mistakenly believe that their own overdose risk is lower than average [7].

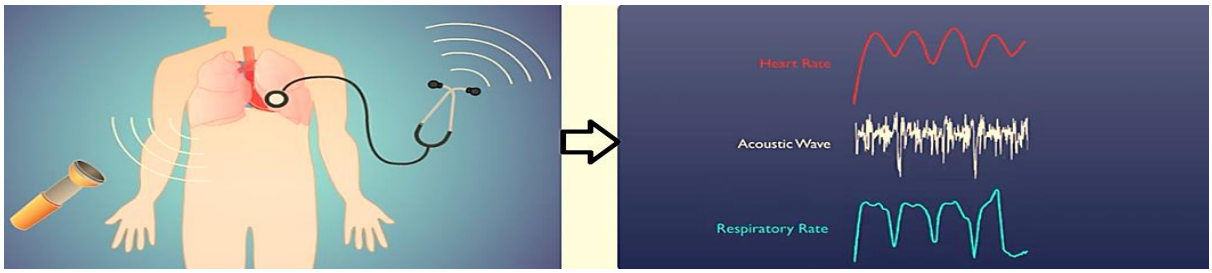

Figure 1: Pill monitoring the gastro and respiratory parameter through signals

Because of this, there are approximately 300,000 nonfatal opioid overdoses annually in along with fatal overdoses. Patients, their caregivers, and healthcare professionals frequently are unaware when a patient is having OIRD when they are not in a medical institution [8]. The chance of experiencing more overdoses—both fatal and nonfatal—increases after one nonfatal overdose. It is known that early intervention increases the likelihood of using opiate antagonists to improve survival. The latest advancements in wearable along with portable device algorithms can facilitate the early identification of respiratory alterations. OSA is characterized by partial (hypopnea) or full (apnea) lung occlusion. A testing facility may diagnose OSA. or by at-home monitoring with the incorporation of sensors that measure oxygen hemoglobin [9], also thoracic, gastrointestinal, and lung function. For mild OSA, surgical procedures, medical devices, and behavioral therapy are available forms of treatment. It is estimated in US, the ailment affects seventeen percent of women and 33.9 percent of men among the age range of 30 and 70. Because of these constraints, the evaluation process's throughput is still restricted, which may burden some of the examined participants. Wearing and connecting to monitoring devices within the home is still necessary for at-home evaluation. Around 80% of moderately severe OSA cases go undetected, despite advancements in at-home screening. For patients with neuromuscular illness, congestive cardiac failure, or chronic obstructive lung disease, this arrangement might not be appropriate. The system setting needs to be more user-friendly and straightforward for the patient's comfort and compliance. Additionally, it was discovered that the current wearable apnea detection techniques have a number of significant shortcomings, including a high price tag, limited capacity to satisfy diagnostic requirements, imprecise findings in aberrations, and difficult usage

in unsupervised environments. In tools that enable remote evaluation could revolutionize how people can be evaluated and diagnosed with OSA [10].

Our report details the creation of a wireless, ingestible equipment that can measure vital signs such as respiration through the human gastrointestinal tract. The device has been validated through preclinical testing in pigs and the first clinical trial in human subjects, in response to these pressing healthcare needs. Our hypothesis was that an electronic device that can be ingested and capture signals in multiple modes would aid in the precise diagnosis and tracking of various ailments that impact the cardiovascular and respiratory systems. We present first assessments conducted in environments linked to opiate overdose and in line with the evaluation of sleep studies.

2. MATERIALS AND METHODOLOGIES

2.1 Electronic Circuit Design and Evaluation

The downsized glucose biofuel cell (BFC) faces challenges with insufficient voltage and power for commercial wireless transmissions. Traditional BFC-powered systems typically use a DC-to-DC converter to address low voltage issues, but this approach exceeds the intended power budget due to large power conditioning circuits and associated losses. To address this, a specially designed microprocessor has been developed, eliminating the need for a DC-DC converter by directly functioning from the BFC [11]. This integrated circuit (IC) employs a volt-to-bandwidth conversion technique with a micro-human body communication (mHBC) transmitting device, achieving an average power consumption of less than 0.4 μW.

The custom-designed circuit operates in two stages. In Phase 1, switch S2 is closed, connecting the BFC to a capacitor, CDD, through the main power supply, VDD. This voltage powers a voltage-controlled oscillator (VCO1) [12], whose frequency varies from 1 to 60 Hz based on VDD. A pulse (Ø1) generated on VCO1's rising edge temporarily shuts off S2 and turns on S1. The BFC is then connected to resistor Rtrack, producing voltage Vtrack, which powers VCO2 and an LC-based mHBC power generator driven by capacitor CDD. The generated signal ranges from 10 kHz to 1 MHz. The produced chip is integrated into a 16.4 × 7.5 mm circuit board, requiring connections to the on-board mHBC antennae and CDD. Circuit measurements demonstrated a quadratic glucose concentration-to-voltage-to-frequency pattern.

2.2 Design and Characterization of Electrochemistry

To address pH variations in the small intestine, the BFC's performance was evaluated over a pH range of 6 to 8. Data indicates that glucose reaction changes with solution pH, with sensor responsiveness improving as pH decreases. Larger signal increases were observed for pH 6 solutions, while pH 8 solutions showed smaller increases. This behavior aligns with expected enzyme production between pH 5.5 and 6.7. The detector's signal also declined with decreasing pH in glucose-absent conditions. The system's capability to generate signals was further tested under various oxygen levels. Using pH 6.8 for typical intestinal oxygen levels, BFC potential changes from 0.586 to 0.386 V at 30 mM glucose across different nitrogen purging durations, indicating an oxygen-glucose reaction relationship. Figure 2 explores the utilized sample handled mechanism.

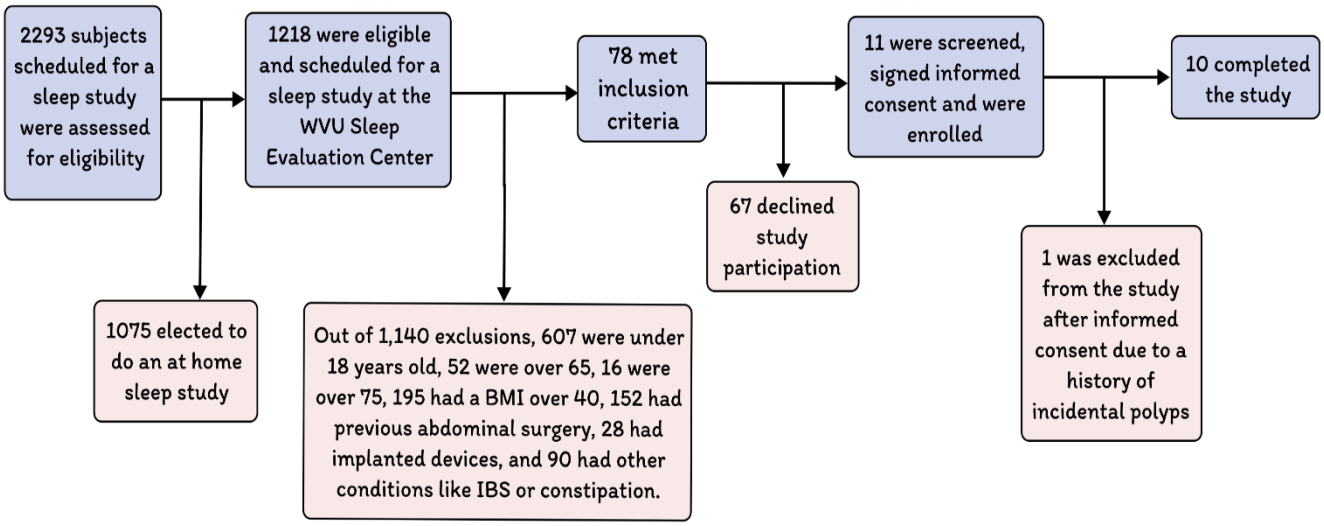

Figure 2: Overall taxonomy of the samples handling

Chronoamperometric responses of the cathode at different oxygen levels showed minimal potential variations (~4 mV) between the two tested O2 levels. Temperature tests conducted at 35, 37, and 39 °C showed minimal sensor reading variations between 35 and 37 °C, with lower readings at 39 °C. For in vitro tests, 37 °C was chosen to consider physiological temperature influence on BFC response. Under these conditions, BFC potential response in glucose solutions (0, 30, 60, and 90 mM) demonstrated good stability and reversibility [13]. A quadratic fitting achieved a coefficient of determination of 0.991. The electrical circuitry requires about 0.4 μW for signal transmission. The BFC's ability to provide sufficient power at all concentrations, even without glucose, was further confirmed by matching power outcomes.

To protect BFCs from acidic digestive juices (pH 1.8) during stomach passage, a pH-responsive mucosal covering was used, remaining intact until BFC disintegration in the neutral gut environment (pH ~6.8). After disintegration, BFCs displayed dose-dependent sensitivity.

A fluidic apparatus with a peristaltic pump simulating capsule passage through the digestive system with regulated pH, moisture, and dry air was constructed. The amplifier detected the rate of signal indicating insulin levels. The computerized process for various glucose solutions resulted in a bidirectional response to alternate glucose levels of 0, 31, and 91 mM. This configuration demonstrated high repeatability across devices using quadratic approximation for glucose level calibration. The glucose sensor's dynamic range and detection limit were 3–90 mM and 4.656 mM, respectively. The implant's frequency response showed modest fluctuations (4 to 7%) when tested in artificial gastrointestinal fluid with 60 mM sucrose. The BFC's specific response to sugar was examined by infusing synthetic intestinal solutions containing 90 mM fructose, 0.01 mM LA, 0.01 mM AA, 0.01 mM UA, and 4 mM NaCh. Frequency values for glucose-free solutions were around 75 kHz, with frequency signals rising to 250 kHz when replaced with 90 mM glucose, followed by a decrease after flushing. Solutions with interfering chemicals yielded frequency values similar to glucose-free solutions, indicating minimal cross-reactivity.

Biofouling was assessed by testing sensor response in artificial stool fluid containing lipids, mucin, bovine albumin serum, poly(acrylic acid), and phosphatidylcholine—major constituents of synthetic mucus under in vitro conditions. Sensor response changed by less than 10% when sugar was added to synthetic liquid mixtures [14,15], indicating capsule functionality despite biofouling substances. Quicker signal shifts in synthetic solutions without artificial mucus were observed due to faster glucose absorption into the device's glucose detector compartment.

2.3 In Vitro Glucose BFC Characterization and Modeling

BFC potential measurements under a 200 kΩ load with 30 mM dextrose at varying oxygen and N2 purging periods were conducted. Four tests were conducted, with the red shaded region representing inter-sample variability. BFC power at various glucose concentrations was measured using linear sweep voltage (scan rate: 5 mV s−1), shown as mean values +/− SD. Horizontal error bars represent inter-sample differences; n = 3 tests were conducted. After activation, the three-layer enteric-coated BFC detector's potential under load responded to varying glucose amounts (0, 10, and 20 mM). The in vitro fluidic system simulation and its operation protocol were established. Frequency response to glucose doses (0, 30, and 90 mM) was measured. The glucose concentration calibration curve relative to mHBC signal frequency was presented as mean values +/− SD. The stability test in artificial intestinal fluid with 60 mM fructose lasted three hours. Electromagnetic interference tests were conducted by injecting artificial intestinal fluid with varying compounds.

2.4 In Situ Performance

A pig model was used to evaluate the self-powered glucose biosensor in situ by administering saline solutions with glucose to simulate meal intake. Capsule position and performance were confirmed through imaging after 14 hours. The animal fasted overnight and consumed the medication orally at t = −14 h. The capsule recorded its initial wireless mHBC signals at t = 0 min, indicating digestive coating dissolution. Real-time intestinal glucose level (IGL) was obtained using the calibration process. BGL was used as a validation method to ensure animal glucose levels varied with glucose ingestion. Capsule progression from the stomach to the small-intestinal region was confirmed by CT scan. The BGL and IGL were monitored for three distinct in situ experiments with oral administration of 360 mL of saline with 60 mM dextrose at t = 30 minutes. The capsule

responded quickly to glucose saline solution, increasing its signal frequency and IGL to plateau at 20–22 mM by t = 90 minutes.

IGL reduction from the original dose is attributed to stomach glucose storage or dilution by intestinal fluid presence. Device capability to distinguish between glucose doses was assessed. The first glucose dose gradually raised IGL to 6 mM, and the second dose increased it to 13 mM. BGL increased from 71 mg/dL at t = 0 to 171 mg/dL over 271 minutes.

The effect of glucose-free meals was examined by administering 360 mL of 60 mM glucose at t = 30 minutes, followed by 360 mL of glucose-free saline at t = 120 minutes. IGL initially rose to 16 mM after glucose solution administration, followed by a delayed signal decline, indicating dilution. The signal fell to 0 mM by t = 300 minutes. The pill responded to glucose consumption reduction with a semi-stable IGL of 4-6 mM at t = 180 min, similar to previous results. BGL rose steadily while IGL declined, indicating continuous glucose absorption from the GI tract into the bloodstream. Device operation was confirmed without solution consumption. With more than 100 mL of intestinal fluid present even during fasting, sufficient glucose is available in the animal for the pill to self-power and communicate. The device maintained over 95% reliability during porcine trials. Detailed graphs of fasting, glucose, and saline consumption trials are available.

2.5 First-in-human clinical study

In the first-ever clinical investigation, the WVU Medicine Sleep Examination Center scheduled 2,293 patients for sleep studies between December 2021 and August 2022. After assessing eligibility (refer to the experimental methods), ten individuals—nine males and one female—were enrolled in the first-in-human pilot clinical trial. Out of the total, 1,075 subjects opted for at-home sleep tests (HSTs), while 1,140 were excluded based on the criteria. The average age and body mass index (BMI) of the participants were 41 years and 32.90 kg/m², respectively, as shown in the demographic and clinical results (Table 1). During the trial, 30% of the patients diagnosed with either obstructive sleep apnea (OSA) or central sleep apnea used bilevel-positive airway pressure (BIPAP) or continuous positive airway pressure (CPAP) devices. Radiograph imaging performed 14 days post-trial confirmed that all subjects had passed the VM pill. No adverse events were reported, including those related to intestinal blockage or the ingestion of the VM tablet. The data from the VM pill, totaling 57 hours across the 10 participants, was successfully transferred wirelessly to the external receiver. Throughout the trial, participants occasionally moved during the night, requiring the sleep technologist to realign the external antenna.

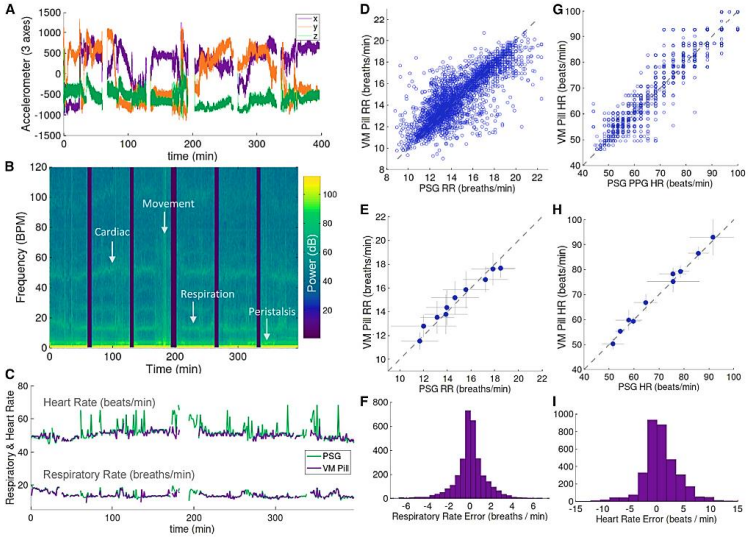

Figure 3: Polysomnography stage assessment in human. (A) A high-level schematic of the VM pill's electronic components.

(B) The VM pill is a compact physiological monitoring device, similar in size to a vitamin (9 x 25 mm), encased in a sealed, biocompatible plastic shell.

(C) The internal components of the VM pill, including two printed circuit boards (PCBs), an antenna, and two silver oxide batteries, are visible within a gel capsule for easy viewing.

(D) The experimental setup designed for testing on pigs.

(E) An example of a y-axis accelerometer signal recorded from the stomach of a pig. (F) Time-frequency spectroscopy of accelerometers illustrating heart and respiration ranges of frequency. Cycles per minute are shown on the y-axis as Hz * 60. (G) A comparison of the respiratory rate (RR) over a 7-minute period between the VM pill and a veterinary lab's vitals monitor (H) A comparison of heart rate (HR) over the same 7-minute period between the VM pill and the lab's vitals monitor, error of 1.6 beats per minute. MCU: microcontroller; Accel: accelerometer.

VM pill accelerometer data (Figure 3A) from the gastrointestinal system shows physiologically appropriate signal frequency ranges (Figure 3B). The combined accelerometer axes are shown in the figure 3B's time-frequency spectrogram. Peristalsis, the most noticeable low-frequency oscillation, was evident in every participant and occurred at a predictable rate of around three waves per minute. The spectrograms of the accelerometer measurements show the respiratory signals as well as sporadic harmonics (Figure 3B), which correspond to expected breathing rates of 9–25 breathes per minute. Furthermore, the cardiac activity as well as its harmonics, which are seen in the 40–95 bpm range, are consistently present in all patients (Figure 3B). Furthermore, the spectrogram shows noticeable peaks at different frequencies that are associated with significant bodily movements (such as turning over in bed or waking up in the middle of the night to use the lavatory). By isolating the signals linked to peristalsis, respiratory, and cardiac frequency bands, signal processing techniques—which are covered in depth in the section on experimental methods—can be utilized to isolate vital indicators such as HR and RR.

During the sleep study, time series measurements of respiratory rate (RR) and heart rate (HR) for subject 001, obtained through the VM pill and polysomnography (PSG), are shown in Figure 3C as an example (refer to Figure 2 for other participants). There are gaps in the data where the signals were not captured, likely due to the wireless transmission process, which took about 5-7 minutes each hour. Additionally, delays in the VM pill data caused by excessive motion or peristalsis were excluded from the study (when PSG data are present).

Comparing the RR estimates from PSG airflow data with the RR accuracy of the VM pill, Figures 3D–3F indicate a difference of only 1 breath per minute. The analysis used 53 hours of data from 10 participants, divided into 1-minute intervals. The mean absolute error between the VM pill RR and PSG RR was 92.7% accurate, with a standard deviation of 1.2 breaths per minute across individuals (7.3%, $p < 0.001$). For a measure less influenced by significant outliers, the mean absolute error was 0.6 breaths per minute (4.3%).Based on the VM pill results, which showed a mean of 14.9 breaths per minute with a variance of 2.1 breaths per minute, the average respiratory rates (RRs) for the 10 participants in the PSG study ranged from 11.5 - 17.7 breaths per minute.

Comparing the heart rate (HR) estimate obtained using the PSG photoplethysmograph (PPG) data with the HR accuracy of the VM pill, Figures 3G–3I indicate a difference of only 2-3 beats per minute. During this study, the same 53 hours of data from each of the 10 individuals were divided into 1-minute intervals. Standard variation of the overall error across individuals was 2.7 bpm, with a mean absolute error of 2.5 bpm (3.8%, $p < 0.001$) between the VM pill HR and PSG HR, indicating 96.2% reliability. 1.5 beats per minute (2.6%) was the average absolute variance.

2.6 CLSTM-based Glucose Data Analysis

The Concatenated Long Short-Term Memory (CLSTM) model is a deep learning architecture designed for temporal sequence analysis. By combining Convolutional Neural Networks (CNNs) with Long Short-Term Memory (LSTM) networks, the CLSTM model can capture spatial and temporal patterns in data. In the context of glucose data analysis, the CLSTM model utilizes the ability of CNNs to identify spatial features in the input data, such as glucose concentrations over time. LSTMs excel at modeling temporal dependencies, enabling the CLSTM model to make accurate predictions and provide valuable insights into glucose trends.

2.6.1 Data Preprocessing

Before applying the CLSTM model, the glucose data undergoes preprocessing to ensure data quality and compatibility with the model. Preprocessing steps may include:

- **Data Cleansing:** Removing missing or erroneous values from the glucose data.
- **Normalizing:** Scaling the glucose concentrations to a consistent range, facilitating convergence during training.

- **Data Segmenting:** Splitting the glucose data into sequences of fixed length, creating input samples for the CLSTM model.

2.6.2 Model Architecture

The CLSTM model's architecture consists of the following components:

- The inputted glucose sequences are processed through a convolutional layer to extract spatial features. This layer captures patterns and trends within the glucose data.
- The retrieval spatial features are passed through an CLSTMs layer, which models the temporal dependencies and relationships between glucose concentrations over time.
- The output of the CLSTMs layer is flattened and passed through a fully connected layer to generate the final prediction. This layer produces the predicted glucose concentration or any other target variable of interest.

2.6.3 Training and Evaluation

The CLSTM model is trained using labeled glucose data, where the input sequences are paired with the corresponding target values. The training process involves optimizing the model's parameters to minimize the prediction error. The evaluation of the CLSTM model's performance is done using validation data, assessing metrics such as RR mean error as in figure 4.

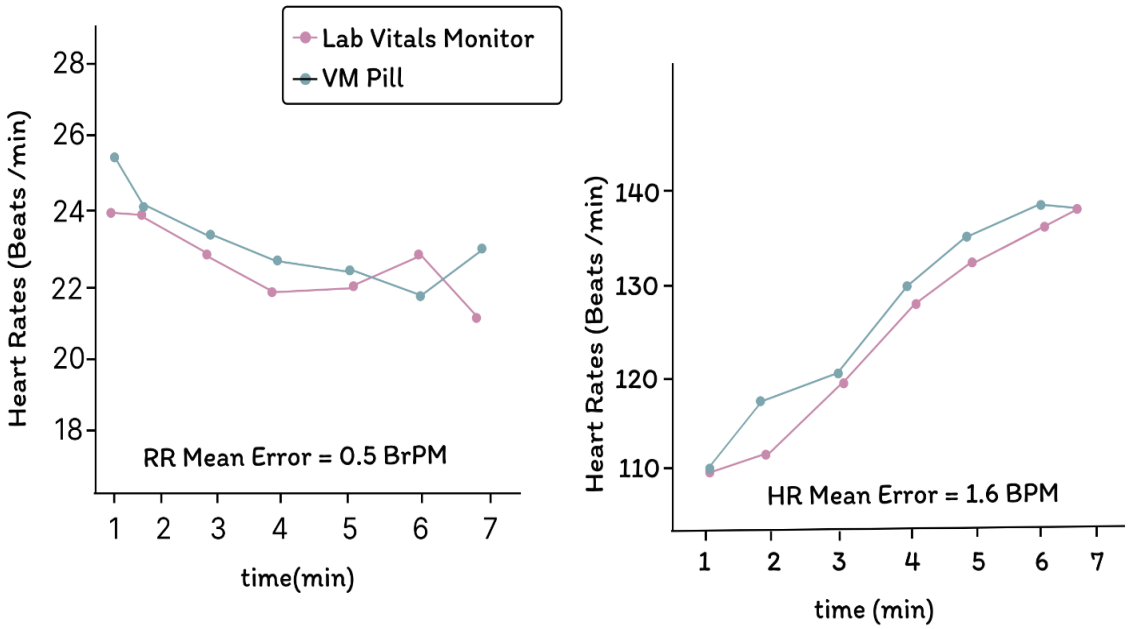

Figure 4: Error rate prediction

The CLSTM model demonstrates high accuracy in predicting glucose concentrations based on historical data. The model's ability to capture spatial and temporal patterns in the glucose data contributes to its superior performance compared to traditional models. The insights gained from the CLSTM analysis provide valuable information for understanding glucose trends and optimizing monitoring strategies. By analyzing the glucose data with the CLSTM model, researchers and healthcare professionals can gain a deeper understanding of glucose dynamics and make informed decisions regarding patient care and treatment plans.

4. EXPERIMENTAL PROCEDURES

4.1 Procedures for swine model experiments

The Cummings School of Veterinary Medicine at Tufts University, located in North Grafton, Massachusetts, USA, was the site of preclinical animal research. These studies examined the capacity to assess vital signs via the gastrointestinal system in pigs. The Institutional Animal Care & Use Committee authorized all study. In the morning of the surgery, the animal was intubated and given midazolam (0.2 mg/kg) and dexmedetomidine (0.03 mg/kg) intramuscularly

VM pill information may be saved in memories and sent in batches to a laptop for offline the process, or they could be broadcast in real time. The HRs & RRs were estimated using the same methods as are detailed next for the examination of clinical information. CVL monitoring apparatus captured HR values from a photoplethysmography (PPG) sensor on the animal's ear and RR readings from a flow detector every 10 seconds. The average of these values was calculated for every non-overlapping one-minute period.

An earlier VM pill used in the opioid overdose study included the same radio, microcontroller, and accelerometer. During sedation, the animal (n = 1) received 250 mg of fentanyl intravenously. Manual help was given sporadically using a rebreathing device when the creature ceased inhaling. Intravenous lidocaine 1 mg reversed the effects of opioid overdose. The stomach-based technology assessed respiration rate (RR) in contemporaneously throughout both the overdose and the recovery process. Utilizing the identical techniques described in the clinical information interpretation section next, the device's microcontroller tallied the entire amount of crossings of zero inside each lung waveform over intervals of fifteen seconds.

An RR, measured in breaths per minute, was calculated based on the zero crossing counts. In both trials, the animal was monitored until it could move around and eat and drink independently. No adverse effects were reported. An RR measured in breaths per minute was created using the zero crossing counts. The device alerted the computer to the presence of OIRD by sending a message titled "overdose detected" if the respiration rate fell below 6 breaths per minute.In both trials, the animal was kept under observation until it could walk around and feed and drink on its own. There were no negative consequences reported.

4.2 Pilot clinical study design

We tested a wireless, consumed gadget in a low-risk, exploratory investigation of healthy adults receiving polysomnography (PSG). This study complied with generally recognized guidelines for optimal clinical conduct in addition to all relevant federal regulations. All 10 subjects gave written informed permission prior to research enrollment.

The research was carried out at the Morgantown, West Virginia, USA-based WVU Medicine Sleeping Assessment the Center, which has everything it needs to identify and manage sleep-related conditions. Utilizing a respiratory inductor plethysmograph and nasal pressures transducer, PSG monitored frontally, essential and parietal neural activity, gaze, breathing, saturation of oxygen, skeletal muscle contractions, and rest heart rate.

The purpose of this study was to compare respiratory signals recorded by the VM pill’s accelerometer with those obtained from polysomnography (PSG) data in participants during sleep or rest. This comparison was designed to evaluate the VM pill's effectiveness in monitoring respiration from within the gastrointestinal tract. Additionally, the study analyzed cardiac signals, comparing data from PSG with data recorded by the VM pill's accelerometer.

Participants in this research were previously enrolled in a sleep study that was planned. After confirming that they're qualified via evaluation by a board-certified gastroenterologist, everybody involved gave written permission. The subjects ingested the VM pill without fasting before beginning their polysomnography (PSG). After getting conventional PSG machinery, the sleep study began. Time-stamped information was gathered and documented all over the participant's sleep duration via the PSG and the VM tablet (The prototype is given in figure 5). About every hour throughout the PSG test, the VM pill sent information for processing to an outside reader.

4.3 Examination of clinical data

Standard polysomnography (PSG) techniques were employed to collect data while the participants were sleeping or resting in bed. After the data were gathered, they were assessed in accordance with the American College of Sleep Medicine's recommendations. Airflow data, captured by a pressure sensor attached to a nasal cannula, and photoplethysmography (PPG) data, collected by an optical sensor attached to the fingertips, were used to provide the "ground truth" for comparison. These served as clinical standards for RRs and HRs respectively.

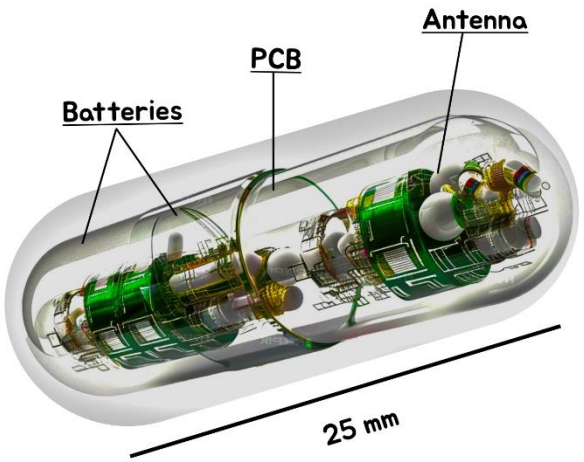

Figure 5: Prototype of the developed pill

To minimize noise, airflow data were separated into one-minute nonoverlapping segments and smoothed using a 20-sample moving average filter. In each window, the number of zero crossings was translated to RR. The PPG information analyzed in the same way, computing HR (beats per minute) by utilizing zero crossings, or locating time points at which the oscillating signal passes zero, in 1-minute frames.

Approximately one hour was dedicated to collecting and storing the VM pill data on the device before it was wirelessly transmitted to a laptop and an external receiver. Sleep technicians manually initiated data transfers, and this process was repeated throughout the duration of the PSG. Occasionally, there were gaps in the data caused by wireless transfer issues. The VM pill's three-axis accelerometer collected data at a rate of 25 hertz (samples per second). Utilizing a non-causal zero-phase delay filter (363636) and a 4th-order Fourier filter (353535), band-limited filtering were utilized to segregate respiratory and cardiovascular signals into their appropriate range of frequencies for each axis. In particular, respiratory impulses were reduced to 0.15–0.42 Hz and cardiac signals to 0.67–1.58 Hz. Within predicted physiologic bounds throughout rest and sleep, these variations in frequency correlate to RR (9–25 breaths per minute).

The heart and breathing band-pass signals were then divided into one-minute, non-overlapping intervals for each axis. The channel in the middle of the gyroscope with the greatest power—which usually had the best signal-to-noise ratio—was utilized to compute RR and HR every one-minute period since the positioning of the sensor changed over time.Each interval has zero crossings found in it. A computation was made of the intervals between zero crossings. Intervals that did not fall within the anticipated physiological limits for RR and HR were eliminated. Each accelerometer axis provided three RR and three HR values for each interval. After applying the aforementioned band-pass filter, the average relative measurement of the electrical signal was measured, and the strength in the cardiac and pulmonary regions was determined at each period. The axis with the greatest power level within the relevant group, which indicates the highest signal-to-noise ratio for the information of interest, was selected to determine the final singular values for RR and HR for that information period.The method used for determining RR and HR excluded intervals with significant movement artifacts. Any noise within the 1.5–4 Hz range present for one minute and exceeding a heuristically determined threshold was classified as a movement artifact interval.

This was due to difficulty in differentiating respiratory waveforms when intervals with heightened peristaltic movement within the respiratory frequency band were removed. Additionally, respiratory rate (RR) and heart rate (HR) computations excluded any period in which the strength of the gyroscope signal exceeded an automatic threshold, ranging from 0.08 to 0.17 Hz.

To facilitate comparison, the datasets were synchronized using timestamps from both the polysomnography (PSG) and VM pill data. Average relative variance among VM pill and PSG information was used to assess RR and HR accuracy. The analysis included both intra- and inter-subject errors in RR and HR. Analyzing each subject's mean absolute deviation after randomized VM pill RR and HR data 1,000 times was required.

5. CONCLUSION AND FUTURE ENHANCEMENTS

In this work, we invented a sophisticated ingestible biological sensing capsule that is battery-free and self-powered, thereby facilitating the real-time measurement of glucose in the intestine. This innovative approach addresses critical challenges associated with conventional ingestible devices, including the elimination of the need for batteries, the miniaturization of electronics, the transmission of signals through dense cellular tissue, and the protection of biosensors from severe in situ conditions. The biofuel cell (BFC) sensor detects glucose with high sensitivity and minimal cross-reactivity with interfering substances, as demonstrated by in vitro simulations. A stable performance was indicated by the minimal signal alteration observed during prolonged frequency observation. The continuous data collected from in situ experiments in pigs confirmed the successful detection of glucose in the intestine, as variations in glucose content from oral solutions corresponded to these changes. The development of an ingestible device for real-time glucose monitoring in the small intestine has the potential to substantially improve our comprehension of glucose absorption and metabolism in healthy individuals, pregnant women, and diabetic patients. By examining the conversion of complex carbohydrates into sugar and the digestion time as a dietary bolus traverses the intestines, this method has the potential to be used to diagnose malabsorptive conditions, including chronic pancreatitis and dumping syndrome. Urine samples, radiological tracers, and glucose tolerance tests are the primary methods used in the current research on obesity, chronic pancreatitis, and dumping syndrome. Nevertheless, these methods are unable to provide real-time information about absorption rates and necessitate a significant quantity of radioactive materials for metabolic rate assessment. The capsule's capabilities will be improved and extant limitations will be addressed through future development. Examples of scenarios that may require an enhanced permeable membrane to prevent sensor displacement include the ingestion of substantial food, which may result in partial obstruction of the sensor's surface. Furthermore, the capsule can be further optimized for precise glucose measurement by incorporating features such as humidity, pH, and oxygen level monitoring. The use of biosensors in porcine models can be used to demonstrate these improvements without the need for general anesthesia. While the current prototype concentrates on the measurement of glucose in solutions, future iterations could include additional sensor front-ends for amperometric or potentiometric detection, which would be powered by the BFC. Sensors and electronic components can be miniaturized to reduce the device's dimensions to those of commercial ingestible devices, which will facilitate simpler passage through the gastrointestinal tract.. This is consistent with the overarching objective of creating sophisticated ingestible sensor tablets that can monitor the digestive system in real time, including pH levels and hydration, through the use of Concatenated Long Short-Term Memory (CLSTM) data analysis. In contrast to expensive and invasive implantable devices, ingestible sensor tablets provide a minimally intrusive, cost-effective alternative. The present investigation introduces a novel sensor that is capable of monitoring the pH levels, gut motility, hydration levels, and electrolyte balance in real time. The CLSTM algorithm facilitates the precise identification of gastrointestinal disorders, dehydration, and electrolyte imbalances, including Crohn's disease and irritable bowel syndrome. Our results indicate that this adaptable sensor is a valuable instrument for the management of gastrointestinal health and the optimization of hydration. It has the potential to enhance overall health management, personalized treatment, and early detection across diverse populations by facilitating timely interventions.

REFERENCES

[1] Yasmin, R., Sarkar, A., Bhattacharyya, S., Majumder, A., Mukherjee, P., & Samanta, H. Smart Pills and Ingestible Sensors for Real-Time Health Monitoring: A Patient Landscape and Over View.

[2] Schuster, K. F., Thompson, C. C., & Ryou, M. (2024). Preclinical study of a novel ingestible bleeding sensor for upper gastrointestinal bleeding. Clinical Endoscopy, 57(1), 73.

[3] Thwaites, P. A., Yao, C. K., Halmos, E. P., Muir, J. G., Burgell, R. E., Berean, K. J., ... & Gibson, P. R. (2024). Current status and future directions of ingestible electronic devices in gastroenterology. Alimentary Pharmacology & Therapeutics, 59(4), 459-474.

[4] Rane, K., Kukreja, G., Deshmukh, S., Kakad, U., Jadhav, P., & Patole, V. (2024). Robotic Pills as Innovative Personalized Medicine Tools: A Mini Review. Recent Advances in Drug Delivery and Formulation: Formerly Recent Patents on Drug Delivery & Formulation, 18(1), 2-11.

[5] Palanisamy, P., Urooj, S., Arunachalam, R., & Lay-Ekuakille, A. (2023). A Novel Prognostic Model Using Chaotic CNN with Hybridized Spoofing for Enhancing Diagnostic Accuracy in Epileptic Seizure Prediction. Diagnostics, 13(21), 3382.
[6] Mitrakos, V., Cummins, G., Tauber, F. J., Cox, B. F., Pavuluri, S. K., Wood, G. S., ... & Desmulliez, M. P. (2024). PressureCap: An endoscopic sensor capsule for real-time gastrointestinal pressure monitoring. Device, 2(5).
[7] You, S. S., Gierlach, A., Schmidt, P., Selsing, G., Moon, I., Ishida, K., ... & Traverso, G. (2024). An ingestible device for gastric electrophysiology. Nature Electronics, 1-12.
[8] Palanisamy, P., Padmanabhan, A., Ramasamy, A., & Subramaniam, S. (2023). Remote patient activity monitoring system by integrating IoT sensors and artificial intelligence techniques. Sensors, 23(13), 5869.
[9] Kulurkar, P., kumar Dixit, C., Bharathi, V. C., Monikavishnuvarthini, A., Dhakne, A., & Preethi, P. (2023). AI based elderly fall prediction system using wearable sensors: A smart home-care technology with IOT. Measurement: Sensors, 25, 100614.
[10] Del-Rio-Ruiz, R., da Silva, D. R. R., Suresh, H., Creasey, H., Asci, C., dos Santos, D. M., ... & Sonkusale, S. (2024). Soft autonomous ingestible device for sampling the small-intestinal microbiome. Device, 100406.
[11] Steiger, C., Abramson, A., Nadeau, P., Chandrakasan, A.P., Langer, R., and Traverso, G. (2018). Ingestible electronics for diagnostics and therapy. Nat. Rev. Mater. 4, 83–98.
[12] Sapra, A., Malik, A., and Bhandari, P. (2022). Vital Sign Assessment (Stat-Pearls).
[13] NPR. U.S. drug overdose deaths hit a record in 2022 as some states see a big surge. https://www.npr.org/2023/05/18/1176830906/overdose-death2022-record.
[14] Office of National Drug Control Policy. The President's Commission on Combatting Drug Addiction and the Opioid Crisis, Final Report. https:// trumpwhitehouse.archives.gov/sites/whitehouse.gov/files/images/Final_ Report_Draft_11-15-2017.pdf.
[15] CDC National Center for Health Statistics. Provisional Counts of Drug Overdose Deaths, as of 8/6/2017. https://www.cdc.gov/nchs/data/ health_policy/monthly-drug-overdose-death-estimates.pdf.